

MedChemComm

Accepted Manuscript

This article can be cited before page numbers have been issued, to do this please use: N. I. Vasilevich, I. Afanasyev, E. Rastorguev, D. Genis and V. Kochubey, *Med. Chem. Commun.*, 2013, DOI: 10.1039/C3MD00211J.



This is an *Accepted Manuscript*, which has been through the RSC Publishing peer review process and has been accepted for publication.

Accepted Manuscripts are published online shortly after acceptance, which is prior to technical editing, formatting and proof reading. This free service from RSC Publishing allows authors to make their results available to the community, in citable form, before publication of the edited article. This *Accepted Manuscript* will be replaced by the edited and formatted *Advance Article* as soon as this is available.

To cite this manuscript please use its permanent Digital Object Identifier (DOI®), which is identical for all formats of publication.

More information about *Accepted Manuscripts* can be found in the [Information for Authors](#).

Please note that technical editing may introduce minor changes to the text and/or graphics contained in the manuscript submitted by the author(s) which may alter content, and that the standard [Terms & Conditions](#) and the [ethical guidelines](#) that apply to the journal are still applicable. In no event shall the RSC be held responsible for any errors or omissions in these *Accepted Manuscript* manuscripts or any consequences arising from the use of any information contained in them.

Dual mode of action of Phenyl-Pyrazole-Phenyl (6-5-6 system) based PPI inhibitors: alpha-helix backbone versus alpha-helix binding epitope.

Natalya I. Vasilevich*, Ilya I. Afanasyev, Eugene A. Rastorguev, Dmitry V. Genis, Valery S. Kochubey

ASINEX Ltd., 20 Geroev Panfilovtsev Str., Moscow 125480, Russia

Protein-protein interactions are involved in regulating a variety of important cellular pathways and inter alia in cancer development. Therefore they represent a highly attractive class of targets for drug discovery, that for a long time were considered as undruggable. However, essential progress has been achieved during recent years, and potent PPI inhibitors such as nutlin-3 and ABT-737 have been developed¹⁻⁶.

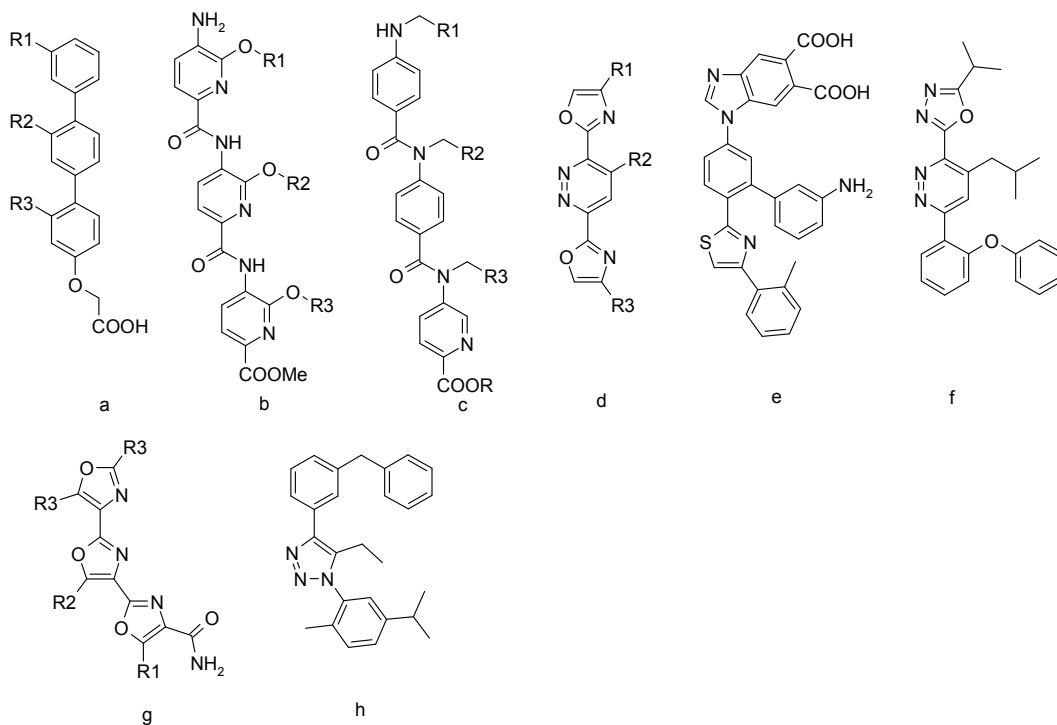
It was suggested that although protein interfaces are large, often a small subset of the residues (so called “hot spots”) contributes significantly to the free energy of binding⁷. These residues can be identified for example by alanine scanning mutagenesis. Analysis of the occurrence of hot spot amino acids in helix-mediated protein interfaces revealed that in most cases they are aromatic tyrosine, phenylalanine and tryptophan, leucine and arginine⁷. Secondly, it was found that the regions in the protein involved in interaction are often organized in alpha-helices that deliver side chains to very definite positions. That means that in order to get small molecule inhibitor aromatic and hydrophobic groups mimicking the residues mentioned above should be placed in a well-defined positions, their relative orientation should be similar to those of the corresponding amino acid substituents in the alpha-helix region. Since most of the “hot spot” residues are located on the one recognition face (60% of all interactions⁷) these sites should correspond to i, i+4 (i+3) and i+7 residues. As an example of such an approach, Fry and coworkers have analyzed alpha-helix epitope and generated a pharmacophore model for mutual orientation of suitable hydrophobic groups⁸.

In the design of small molecule antagonists capable of interrupting protein-protein interactions two kinds of approaches are generally employed: alpha-helix backbone mimetic and alpha-helix binding epitope mimetic design (mimetics of both types are exemplified in Figure 1). Both of these approaches proved to be successful. The difference between them is that while the first approach includes design of scaffolds that mimic alpha-helix backbones and side substituents occupy positions corresponding to the “hot spots”, the second one do not utilize alpha-helix backbones but uses any core (often any heterocycle) that can place hydrophobic substituents in

appropriate positions. Both models have their inherent drawbacks: difficult and multi-step synthesis for the first model and deviation in side chain vector orientation from the vector in natural alpha-helices for the second one. Both tend to have poor solubility and ADME properties requiring solubilizing group incorporation.

However, sometimes assigning a scaffold to one of these types is not so obvious. Especially this regards the scaffolds containing five-member heterocycle in the central position like scaffolds **g**⁹ and **h**¹⁰ (Figure 1). In accordance with the reported calculations and crystallographic data these scaffolds can adopt a conformation that mimic the alpha-helix backbone. On the other hand presence of the central five-member ring makes the molecule slightly bent and the core of compound **h** clearly resembles the core of the classical epitope mimetic nutlin. However, in contrast to nutlin central heterocycle in **h** is fully aromatic and doesn't allow any translatory motion but only rotation. Unfortunately there is no data about biological activity of scaffolds **g** and **h** against PPI targets in the literature.

Alpha-helix backbone mimetics



Alpha-helix binding epitope mimetics

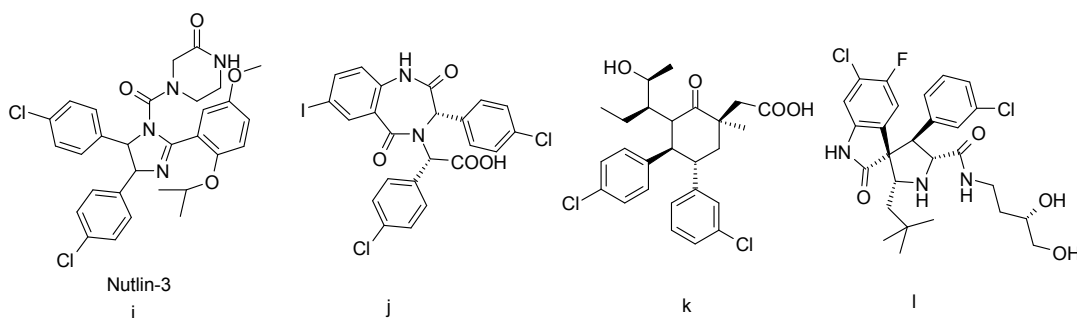


Figure 1. Examples of two types of small molecule antagonists of PPIs: α -helix backbone mimetics and α -helix epitope binding mimetics

In the present report we suggest a novel scaffold containing five-member cycle in the central position that we assume to be able serving as both an alpha-helix backbone mimetic and an alpha-helix binding epitope mimetic depending on the nature of substituents (Figure 2).

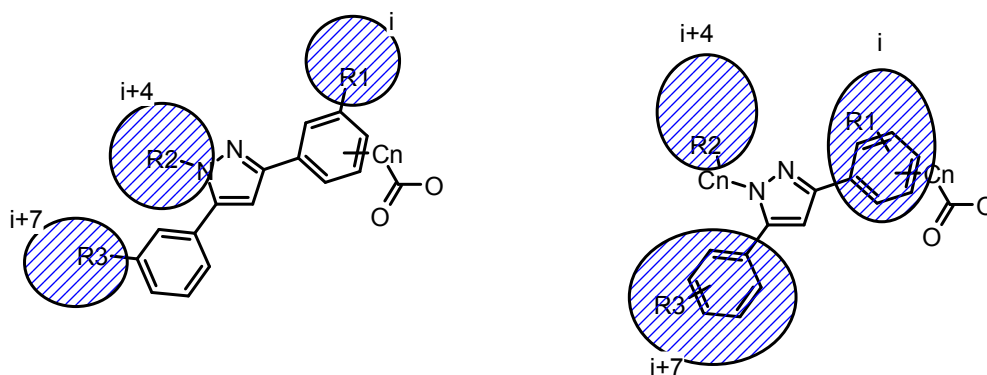


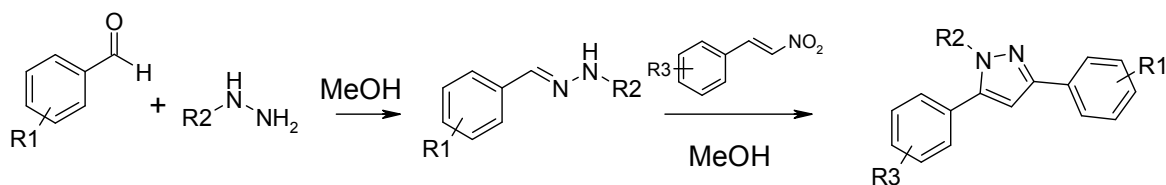
Figure 2. Two modes of interaction assumed for compounds of the new scaffold with *i*, *i*+4 and *i*+7 subpockets

We suppose that when R_1 and R_3 groups are large and hydrophobic this scaffold acts as an alpha-helix mimetic and the phenyl-pyrazole-phenyl core mimics the alpha-helix backbone; and when R_1 and R_3 groups are quite small the scaffold acts as epitope mimetic and both terminal phenyl groups occupy subpockets corresponding to side chains of *i* and *i*+7 residues in the α -helix.

In addition, a carboxy-group connected to one of the phenyl rings, directly or through a C_n linker was introduced. This carboxy-group can extend the value of our scaffold due to several reasons. Firstly it can serve as a solubilizing group. Secondly, the carboxy group is known to be overrepresented among PPI ligands¹¹, so this group might potentially participate in additional interaction with the target. And finally, in accordance with our computer modeling the carboxy group can serve as a synthetic handler that allows the introduction of an additional group corresponding to *i*+11 residues.

We elaborated a very feasible and straightforward “one pot” synthetic procedure resulting in the creation of a library in a timely and cost effective manner. As a central ring the pyrazole moiety was chosen as it is a privileged fragment in medicinal chemistry. It is well known that the synthesis of substituted pyrazoles is prone to result in a mixture of regioisomers. However a method was published recently that describes the synthesis of pyrazoles from *N*-arylhydrazones and nitroolefins in a high yield and excellent regioselectivity^{12,13}. We applied this new method to the synthesis of a medium size library of 52 compounds (Scheme 1). A solution of hydrazine salt in methanol was added to equimolar amount of aldehyde in methanol. After stirring at room temperature for 1 hour a solution of β -nitro-styrene (0.9 eq.) in methanol was added and the reaction mixture was stirred at room temperature for an additional 24 hours followed by chromatographic purification of the final product. It is worth mentioning that using di-substituted nitro-olefines instead of nitrostyrenes allows the introduction of fourth substituents in the

pyrazole ring, which can be used for example as an additional solubilizing group (data not shown).



Scheme 1. Synthetic scheme for the preparation of phenyl-pyrazole-phenyl based compounds.

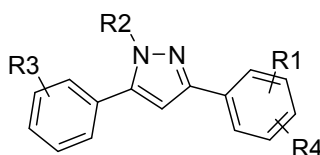
More than 80% of the compounds obtained meet the descriptor requirements favorable for PPI inhibitors such as SHP2, Mor11m, dipole, RDF070m, and Ui suggested in the literature¹⁴⁻¹⁶ (see supporting information) and show satisfactory solubility in PBS buffer (38% of compounds possess kinetic solubility > 0.2 $\mu\text{M}/\text{mL}$). Molecular weights of the compounds were within the range from 373 to 597 Da.

As a model of protein-protein interaction the MDM2-p53 interaction was chosen. All synthesized compounds were tested in the MDM2-p53 binding assay using a commercially available truncated p53 (17-26) containing the p53 binding domain. Truncation to residues 17–26 increases affinity to MDM2 13-fold comparing to wild-type p53 peptide¹⁷. As a consequence the IC_{50} of nutlin-3, used as a reference in our assay, appeared to be 474 nM instead of 90 nM quoted in the literature¹⁵. The results of the biological testing are given in Table 1 in comparison with nutlin-3.

It was found that 8 compounds possess IC_{50} less than 30 μM , so the designed library possesses relatively high hit rate of 15%. Ligand efficiencies for these compounds ranges from 0.12 to 0.21, so they are comparable with the ligand efficiency of nutlin-3 in our assay (0.22) and are very good for the library targeted on PPIs^{1, 18}.

Looking at the Table 1 one can see that the most active compounds contain carboxylic group linked to phenyl ring directly, elongation of the linker to CH_2COOH leads to ten-fold less active compounds (compare **1** and **18**, **2** and **19**). Among two tested N-pyrazole substituents (R^2) longer and more flexible phenethyl is better than benzyl. Phenyl-pyrazole-phenyl based compounds appeared to be quite sensitive to R^3 substituents: while methoxy derivative **34** possessed IC_{50} 185 μM , more lipophilic ethoxy (**4**), propoxy (**1**), butoxy (**5**), and isobutoxy (**2**) derivatives were among the most active compounds.

Table 1. Biological data for compounds of general formula



nn	R1	R2	R3	R4	MDM2/p53, IC ₅₀ μM	LE	Solubility, Ug/mL
1	2-OC ₃ H ₇	-C ₂ H ₄ Ph	2-OMe, 3-OMe	5-COOH	6.56	0.20	0.117
2	2-OCH ₂ CH(CH ₃) ₂	-C ₂ H ₄ Ph	2-OMe, 3-OMe	5-COOH	8.22	0.19	0.056
3	2-OEt	-C ₂ H ₄ Ph	2-OEt	5-COOH	10.65	0.21	0.022
4	2-OEt	-C ₂ H ₄ Ph	2-OMe, 3-OMe	5-COOH	13.98	0.20	>0.2
5	2-OC ₄ H ₉	-C ₂ H ₄ Ph	2-OMe, 3-OMe	5-COOH	14.15	0.19	0.066
6	2-OCH ₂ CH(CH ₃) ₂	-C ₂ H ₄ Ph	2-OEt	5-COOH	14.19	0.19	0.015
7	2-OC ₄ H ₉	-C ₂ H ₄ Ph	2-OEt	5-COOH	16.75	0.19	0.032
8	2-OMe	-CH ₂ Ph	4-F	5-C ₂ H ₄ COOH	16.98	0.21	0.066
9	2-OCH ₂ (3-Cl-Ph)	-CH ₂ Ph	2-OMe, 3-OMe	5-C ₂ H ₄ COOH	31.62	0.15	<0.015
10	2-OCH ₂ (3-Cl-Ph)	-C ₂ H ₄ Ph	2-OMe, 3-OMe	5-C ₂ H ₄ COOH	34.02	0.15	<0.015
11	2-OEt	-C ₂ H ₄ Ph	4-F	5-C ₂ H ₄ COOH	35.78	0.18	>0.2
12	2-OMe	-C ₂ H ₄ Ph	4-Cl	5-C ₂ H ₄ COOH	38.87	0.19	0.046
13	2-OCH ₂ (3-Cl-Ph)	-C ₂ H ₄ Ph	4-F	5-C ₂ H ₄ COOH	47.83	0.15	<0.015
14	2-OCH ₂ CH(CH ₃) ₂	-C ₂ H ₄ Ph	2-OEt	5-CH ₂ COOH	48.7	0.16	0.046
15	2-OCH ₂ (3-Cl-Ph)	-CH ₂ Ph	4-F	5-C ₂ H ₄ COOH	51.88	0.16	<0.015
16	2-OC ₄ H ₉	-C ₂ H ₄ Ph	2-OEt	5-CH ₂ COOH	54.06	0.16	0.096
17	2-OCH ₂ (3-Cl-Ph)	-CH ₂ Ph	2-OEt	5-CH ₂ COOH	54.39	0.15	<0.015
18	2-OC ₃ H ₇	-C ₂ H ₄ Ph	2-OMe, 3-OMe	5-CH ₂ COOH	60.6	0.16	0.117
19	2-OCH ₂ CH(CH ₃) ₂	-C ₂ H ₄ Ph	2-OMe, 3-OMe	5-CH ₂ COOH	68.32	0.15	0.056
20	2-OC ₃ H ₇	-CH ₂ Ph	2-OEt	5-COOH	68.75	0.17	0.096
21	2-OC ₃ H ₇	-C ₂ H ₄ Ph	2-OEt	5-CH ₂ COOH	71.98	0.16	0.066
22	2-OC ₃ H ₇	-CH ₂ Ph	2-OMe, 3-OMe	5-COOH	79.27	0.17	>0.2
23	2-OMe	-CH ₂ Ph	4-Cl	5-C ₂ H ₄ COOH	86.63	0.18	0.019
24	H	-C ₂ H ₄ Ph	2-OEt	4-COOH	91.22	0.18	>0.2
25	2-OEt	-CH ₂ Ph	4-F	5-C ₂ H ₄ COOH	100.8	0.17	<0.015
26	2-OEt	-C ₂ H ₄ Ph	2-OEt	5-CH ₂ COOH	102.4	0.16	>0.2
27	2-OEt	-C ₂ H ₄ Ph	2-OEt	5-C ₂ H ₄ COOH	105.4	0.16	0.102
28	2-OEt	-CH ₂ Ph	2-OEt	5-COOH	111.1	0.17	0.066
29	2-OC ₄ H ₉	-C ₂ H ₄ Ph	2-OMe, 3-OMe	5-CH ₂ COOH	115.6	0.15	0.117
30	2-OC ₄ H ₉	-CH ₂ Ph	2-OMe, 3-OMe	5-CH ₂ COOH	117.7	0.15	>0.2
31	2-OCH ₂ CH(CH ₃) ₂	-CH ₂ Ph	2-OMe, 3-OMe	5-CH ₂ COOH	120.0	0.15	>0.2
32	H	-C ₂ H ₄ Ph	4-F	4-COOH	127.9	0.2	0.096
33	2-OCH ₂ (2-Cl-Ph)	-CH ₂ Ph	4-F	5-CH ₂ COOH	129.8	0.14	<0.015
34	2-OMe	-C ₂ H ₄ Ph	2-OMe, 3-OMe	5-COOH	185.6	0.15	>0.2
35	2-OMe	-C ₂ H ₄ Ph	2-OEt	5-COOH	232.5	0.16	>0.2
36	2-OMe	-CH ₂ Ph	2-OEt	5-COOH	238	0.16	0.039
37	2-OCH ₂ (3-Cl-Ph)	-C ₂ H ₄ Ph	2-OEt	5-CH ₂ COOH	248.8	0.12	<0.015
38	2-OMe	-C ₂ H ₄ Ph	2-OEt	5-C ₂ H ₄ COOH	258.4	0.14	>0.2
39	2-OMe	-CH ₂ Ph	2-OEt	5-CH ₂ COOH	287.6	0.15	0.138

40	2-OEt	-CH ₂ Ph	2-OMe, 3-OMe	5-COOH	294.5	0.15	0.138
41	2-OC ₃ H ₇	-CH ₂ Ph	2-OMe, 3-OMe	5-CH ₂ COOH	328.6	0.14	>0.2
42	2-OMe	-C ₂ H ₄ Ph	2-OEt	5-CH ₂ COOH	339.2	0.14	>0.2
43	H	-CH ₂ Ph	2-OEt	4-COOH	346.4	0.16	0.117
44	2-OEt	-CH ₂ Ph	2-OMe, 3-OMe	5-CH ₂ COOH	348.2	0.14	>0.2
45	2-OEt	-CH ₂ Ph	2-OMe, 3-OMe	5-C ₂ H ₄ COOH	352.7	0.14	>0.2
46	2-OMe	-CH ₂ Ph	2-OEt	5-C ₂ H ₄ COOH	388.1	0.14	>0.2
47	2-OMe	-C ₂ H ₄ Ph	2-OMe, 3-OMe	5-C ₂ H ₄ COOH	436.5	0.13	>0.2
48	2-OMe	-CH ₂ Ph	2-OMe, 3-OMe	5-C ₂ H ₄ COOH	449.2	0.14	0.169
49	2-OMe	-CH ₂ Ph	4-F	5-CH ₂ COOH	594.7	0.15	>0.2
50	2-OMe	-C ₂ H ₄ Ph	2-OMe, 3-OMe	5-CH ₂ COOH	726.8	0.13	>0.2
51	2-OMe	-CH ₂ Ph	2-OMe, 3-OMe	5-CH ₂ COOH	967.3	0.13	>0.2
52	2-OMe	-CH ₂ Ph	2-OMe, 3-OMe	5-COOH	1018.0	0.13	>0.2
Nutlin-3					0.474	0.22	

To prove our hypothesis about the possibility of a dual mode of interaction with MDM2, a docking study of two active compounds (**8** and **13**) into the MDM2 binding site of the MDM2 complex with p53 (PDB entry 1ycr) was performed. These compounds were chosen because they contain the smallest (**8**) and the bulkiest (**13**) R³ substituents in the library and therefore may adopt either alpha-helix backbone-like or nutlin-like modes of action the best way. As it is seen at Figure 3, we found that depending on their substituents, these compounds (in yellow) may act either as alpha-helix backbone mimetics (left pane, in comparison with p53 – in purple) or alpha-helix binding epitope mimetics (right pane: in comparison with nutlin-2). It seems to be very interesting that in both cases the compounds were docked into complexes with the transactivation domain of p53, but in the first case the optimal conformation seems to be alpha-helix-like, while in the latter case it is obviously nutlin-like.

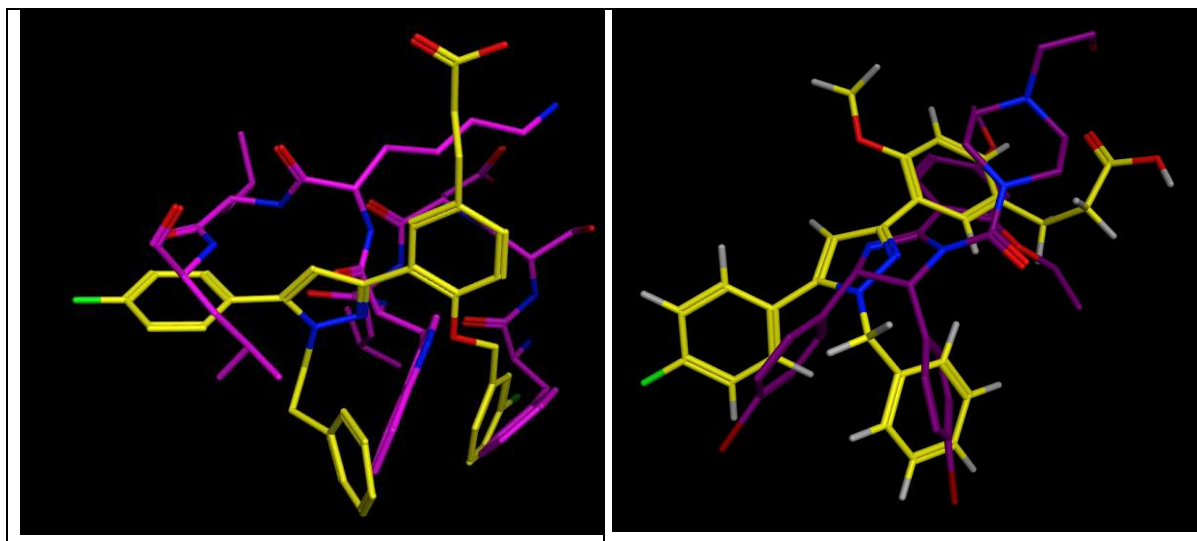




Figure 3. Docking of compounds 8 and 13 into the MDM2 p53 binding site. Left pane: Compound 13 was docked into the p53 binding site of PDB entry 1ycr. Compound 13 (yellow) and transactivation domain of p53 from this entry (purple) are shown. Right pane: Compound 8 was docked into the same complex as in the left pane. MDM2, with 8 docked into it, was then superposed onto the MDM2 complex with nutlin-2 (PDB entry 1rv1). Compound 8 (yellow) and nutlin-2 (purple) are shown.

Compounds from our library were also partially tested against Bcl-xl target and some of them showed activity in 120-600 μM range (data not shown) that could confirm our assumption of possible optimization of this scaffold toward various kinds of PPI targets.

The key point of this work is that very good ligand efficiency was achieved, whilst maintaining relatively low average molecular weight of the compounds in the library. A typical molecular weight for drug candidates targeting PPIs is known to be 700-800 Da¹⁸. This means that the compounds from this work can be considered as starting points for further optimization of properties for targeting various kinds of PPI's, in other words this library allows room for improvement.

Experiment

LCMS were recorded on Surveyor MSQ (Thermo Fisher Scientific) using Phenomenex Onyx Monolythic C18 25X4.6 mm Part No: CHO-7645 column and a gradient from 100% to 5% of mobile phases A (0.1% solution of formic acid in water) in mobile phase B (0.1% solution of formic acid in acetonitrile), flow rate was 1.5 ml/min. Detection was performed using two types of detectors: PDA -photodiode array detector in 200-800 nm range and APCI (+ or - ions) - atmospheric pressure chemical ionization. Total run time -4.5 min, injection volume 2 μL .

The ¹H and ¹³C NMR spectra were recorded in CDCl₃, using TMS as an internal standard, on a Varian Mercury console -400 NMR spectrometer, operating at 400 MHz for ¹H and 100 MHz for ¹³C.

Compounds were purified by HPLC on Agilent 1200 HPLC Instrument. Experimental conditions: column: Luna® 5 μm C18(2) Axia packed (50 x 21.2 mm), mobile phase: A = 0.1 % HCOOH in water, B = 0.1 % HCOOH in acetonitrile, gradient: 1 minute at 98:2 (A/B), to 25:75 (A/B) over 8 minutes, flow rate: 60 mL/min, detection: UV @ 270 nm, injection volume: 400 μL .

Methanol 99.8% (Aldrich) was used and a solvent and acetonitrile LC-MS Chromasolv (Fluka) was used for HPLC purification. Aldehydes were prepared via alkylation of methyl 3-formyl-4-hydroxybenzoate (Aldrich, CAS 24589-99-9) using corresponding alkyl chlorides or alkyl

bromides and potassium carbonate base in DMF. All nitrostyrenes, benzyl-hydrazine hydrochloride and phenethyl-hydrazine were purchased from Aldrich.

3-(5-(2,3-Dimethoxyphenyl)-1-phenethyl-1H-pyrazol-3-yl)-4-propoxybenzoic acid (1)

Phenethylhydrazine hydrochloride (MW 136, 34 mg, 0.25 mmol, 1 eq.) in methanol (0.6 ml) was added to a solution of methyl 3-formyl-4-propoxybenzoate (MW 222, 56 mg, 0.25 mmol, 1 eq.) in methanol (0.6 ml). After stirring at room temperature for 1 h, 2,3-dimethoxy nitrostyrene (MW 209, 47 mg, 0.225 mmol, 0.90 equiv.) was added in methanol (0.6 ml) and the reaction solution was stirred open to air at room temperature for 24 h. To hydrolyze the methyl ester to corresponding benzoic acid 0.2 ml of 20% NaOH solution was added and the reaction mixture was refluxed for 1 h. After acidifying to pH 7 resulting mixture was concentrated and purified by HPLC to give a white solid (40 mg, 37% for two steps). m.p. 86⁰C, ¹H NMR, δ (CDCl₃), ppm: 1.0 (3H, t, J=7Hz); 1.9 (2H, m); 3.2 (2H, t, J=7Hz); 3.62 (3H, s); 3.92 (3H, s); 4.12 (2H, t, J=7Hz); 4.35 (2H, t, J=7Hz); 6.62 (1H, dd, J=8.5Hz/3Hz); 6.80 (1H, s); 7.0 (5H, m); 7.15 (3H, m); 8.12 (1H, dd, J=8.5Hz/3Hz); 8.9 (1H, d, J=3Hz). ¹³C NMR, δ (CDCl₃), ppm: 170.35; 160.36; 153.04; 147.30; 146.56; 140.21; 138.74; 131.30; 131.10; 129.94; 128.33; 126.27; 125.48; 123.90; 123.50; 122.76; 122.24; 113.40; 111.73; 108.20; 70.37; 60.73; 56.10; 51.28; 36.75; 22.64; 10.70. LC-MS *m/z*: 487 (M+H⁺), purity: 95%.

3-(5-(2,3-Dimethoxyphenyl)-1-phenethyl-1H-pyrazol-3-yl)-4-isobutoxybenzoic acid (2)

was synthesized as described for **1** using phenethylhydrazine hydrochloride (MW 136, 34 mg, 0.25 mmol, 1 eq.), methyl 3-formyl-4-isobutoxybenzoate (MW 236, 59 mg, 0.25 mmol, 1 eq.) and 2,3-dimethoxy nitrostyrene (MW 209, 47 mg, 0.225 mmol, 0.90 equiv.) as starting materials. Yield 60 mg, 53% for two steps. m.p. 87⁰C, ¹H NMR, δ (CDCl₃), ppm: 1.01(6H, d, J=7Hz); 2.25 (1H, m); 3.20 (2H, t, J=7Hz); 3.62 (3H, s); 3.92 (5H, m); 4.35 (2H, t, J=7Hz); 6.6 (1H, dd, J=8.5Hz/3Hz); 6.8 (1H, s); 7.0 (5H, m); 7.15 (3H, m); 8.0 (1H, dd, J=8.5Hz/3Hz); 8.90 (1H, d, J=3Hz). ¹³C NMR, δ (CDCl₃), ppm: 170.22; 160.47; 153.03; 147.26; 146.61; 140.24; 138.75; 131.43; 131.14; 128.93; 128.33; 126.23; 125.48; 123.91; 123.50; 122.83; 122.14; 113.39; 111.69; 108.21; 75.32; 60.71; 56.10; 51.29; 36.37; 28.42; 19.42. LC-MS *m/z*: 501 (M+H⁺), purity: 95%.

3-(5-(2,3-Dimethoxyphenyl)-1-phenethyl-1H-pyrazol-3-yl)-4-ethoxybenzoic acid (4)

was synthesized as described for **1** using phenethylhydrazine hydrochloride (MW 136, 34 mg, 0.25 mmol, 1 eq.), methyl 3-formyl-4-ethoxybenzoate (MW 208, 52 mg, 0.25 mmol, 1 eq.) and 2,3-dimethoxy nitrostyrene (MW 209, 47 mg, 0.225 mmol, 0.90 equiv.) as starting materials. Yield 50 mg, 47% for two steps. m.p. 172⁰C, ¹H NMR, δ (CDCl₃), ppm: 1.5 (3H, t, J=7Hz); 3.20 (2H,

t, J=7Hz); 3.65 (3H, s); 3.92 (3H, s); 4.25 (2H, q, J=7Hz); 4.35 (2H, t, J=7Hz); 6.62 (2H, dd, J=8.5Hz/3Hz); 6.8 (1H, s); 7.0 (5H, m); 7.15 (3H, m); 8.15 (1H, dd, J=8.5Hz/3Hz); 8.98 (1H, d, J=3Hz). ¹³C NMR, δ (CDCl₃), ppm: 170.31; 160.21; 153.06; 147.32; 146.50; 140.19; 138.74; 131.25; 131.08; 128.94; 128.34; 126.24; 125.48; 123.89; 123.50; 122.74; 122.28; 113.42; 111.79; 108.23; 64.35; 60.76; 56.10; 51.28; 36.75; 14.79. LC-MS *m/z*: 473 (M+H⁺), purity: 95%.

3-(5-(2,3-Dimethoxyphenyl)-1-phenethyl-1H-pyrazol-3-yl)-4-butoxybenzoic acid (5) was synthesized as described for **1** using phenethylhydrazine hydrochloride (MW 136, 34 mg, 0.25 mmol, 1 eq.), methyl 3-formyl-4-butoxybenzoate (MW 236, 59 mg, 0.25 mmol, 1 eq.) and 2,3-dimethoxy nitrostyrene (MW 209, 47 mg, 0.225 mmol, 0.90 equiv.) as starting materials. Yield 47 mg, 42% for two steps. m.p. 140⁰C, ¹H NMR, δ (CDCl₃), ppm: 0.95 (3H, t, J=7Hz); 1.5 (2H, m); 1.85 (2H, m); 3.2 (2H, t, J=7Hz); 3.62 (3H, s); 3.95 (3H, s); 4.13 (2H, t, J=7Hz); 4.35 (2H, t, J=7Hz); 6.65 (1H, dd, J=8.5Hz/3Hz); 6.8 (1H, s); 7.0 (5H, m); 7.15 (3H, m); 8.12 (1H, dd, J=8.5Hz/3Hz); 8.98 (1H, d, J=3Hz). ¹³C NMR, δ (CDCl₃), ppm: 170.19; 160.38; 153.04; 147.30; 146.55; 140.22; 138.75; 131.31; 131.10; 128.93; 128.33; 126.23; 125.50; 123.90; 123.51; 122.79; 122.16; 113.42; 111.72; 108.19; 64.48; 60.72; 56.11; 51.29; 36.74; 31.31; 19.35; 13.73. LC-MS *m/z*: 501 (M+H⁺), purity: 95%.

3-(5-(2-Ethoxyphenyl)-1-phenethyl-1H-pyrazol-3-yl)-4-isobutoxybenzoic acid (6) was synthesized as described for **1** using phenethylhydrazine hydrochloride (MW 136, 34 mg, 0.25 mmol, 1 eq.), methyl 3-formyl-4-isobutoxybenzoate (MW 236, 59 mg, 0.25 mmol, 1 eq.) and 2-ethoxy nitrostyrene (MW 193, 44 mg, 0.225 mmol, 0.90 equiv.) as starting materials. Yield 59 mg, 54% for two steps. m.p. 205⁰C, ¹H NMR, δ (CDCl₃), ppm: 1.0 (6H, d, J=7Hz); 1.3 (3H, t, J=7Hz); 2.2 (1H, m); 3.2 (2H, t, J=7Hz); 3.92 (2H, d, J=7Hz); 4.05 (2H, q, J=7Hz); 4.35 (2H, t, J=7Hz); 6.75 (1H, s); 7.0 (6H, m); 7.15 (3H, m); 7.37 (1H, t, J=8.5Hz); 8.12 (1H, d, J=8.5Hz); 8.8 (1H, d, 3Hz). ¹³C NMR, δ (CDCl₃), ppm: 170.06; 160.44; 156.46; 146.57; 140.96; 138.81; 131.95; 131.39; 131.03; 130.19; 128.86; 128.34; 126.22; 122.83; 122.28; 120.65; 120.61; 112.64; 111.72; 108.28; 75.34; 64.27; 51.20; 36.87; 28.41; 19.45; 14.77. LC-MS *m/z*: 485 (M+H⁺), purity: 95%.

3-(5-(2-Ethoxyphenyl)-1-phenethyl-1H-pyrazol-3-yl)-4-butoxybenzoic acid (7) was synthesized as described for **1** using phenethylhydrazine hydrochloride (MW 136, 34 mg, 0.25 mmol, 1 eq.), methyl 3-formyl-4-butoxybenzoate (MW 236, 59 mg, 0.25 mmol, 1 eq.) and 2-ethoxy nitrostyrene (MW 193, 44 mg, 0.225 mmol, 0.90 equiv.) as starting materials. Yield 49 mg, 45% for two steps. m.p. 184⁰C, ¹H NMR, δ (CDCl₃), ppm: 0.98 (3H, t, J=7Hz); 1.35 (3H, t, J=7Hz); 1.55 (2H, m); 1.88 (2H, m); 3.15 (2H, t, J=7Hz); 4.05 (2H, q, J=7Hz); 4.15 (2H, t,

J=7Hz); 4.35 (2H, t, J=7Hz); 6.75 (1H, s); 7.0 (6H, m); 7.18 (3H, m); 7.40 (1H, t, J=8.5Hz); 8.10 (1H, dd, J=8.5Hz/3Hz); 8.98 (1H, d, J=3Hz). ¹³C NMR, δ (CDCl₃), ppm: 169.98; 160.35; 156.45; 146.52; 140.96; 138.81; 131.97; 131.28; 130.99; 130.20; 128.86; 128.35; 126.22; 122.81; 122.25; 120.64; 120.60; 112.61; 111.75; 108.26; 68.51; 64.26; 51.22; 36.86; 31.31; 19.35; 14.79; 13.75. LC-MS *m/z*: 485 (M+H⁺), purity: 93%.

Data for LC-MS, yields and purity of other compounds are given in supporting materials.

Biological testing

Test compounds in DMSO were diluted in Assay Buffer (10 mM PBS, pH 7.4, 2 mM DTT, 0.1 mg/ml BGG, 0.01% Triton X-100). An aliquot was transferred into 96-well polypropylene microplates (Corning, 3915) and mixed with 0.2 μ M (final concentration) of 6His-MDM2 (amino acids 1-118; in house). The samples were incubated at room temperature (RT) for 10 min, and then 10 nM (final concentration) of FITC-p53 (amino acids 17-26) (Anaspec, 62386) was added. The samples were incubated at RT for 30 min and FP (fluorescence polarization) was read on a TECAN Infinite F500 (Ex485/Em535).

Molecular docking

The crystal structure of MDM2 complex with p53 was obtained from RCSB protein data bank. Compounds 8 and 13 were docked into the binding site of MDM2 using MOE docking module with London dG scoring function¹⁹. The binding site was determined as the residues of MDM2 at the nearest distance (within 4.5 Å) from p53 residues from Phe19 to Leu26. To further guarantee the appropriate scoring the additional pharmacophore constraint was generated – one hydrophobic center of every docked compound should be positioned in the Trp23-binding region of MDM2. Best scoring conformations were chosen for each compound.

Conclusions

A new class of alpha-helix mimetics, based on the phenyl-pyrazole-phenyl (6-5-6 system), has been designed and synthesized. The ability of the new compounds to inhibit PPIs was exemplified in the MDM2-p53 binding assay. The library revealed an excellent hit rate of 15%, has satisfactory physico-chemical properties (~38% soluble compounds) and ligand efficiency of the best compound was found to be 0.21 (compared to 0.22 for nutlin-3 in the same assay). Dual mode of action of these inhibitors was suggested based on computer modeling: depending on the nature of substituents they could act as either an alpha-helix backbone mimetics or alpha-helix binding epitope mimetics.

A new feasible one-pot synthetic strategy comprising regioselective synthesis of substituted pyrazoles has been applied and adopted for the library synthesis. Bearing in mind the rather

small molecular weights of the new compounds in terms of PPI inhibitor properties they can be considered as starting points for further optimization of properties towards improving activity and selectivity against various kinds of PPIs.

Acknowledgement. We thank Dr. Vitaly Skosyrev for his help in biological experiment performance.

References

1. Fry, D.C. *Current Protein and Peptide Science* 2008, **9**, 240-247.
2. Azzarito, V.; Long, K.; Murphy, N.S. and Wilson, A.J. *Nature Chemistry* 2013, **5**, 161-173.
3. Yin, H.; Lee, G.-I. and Hamilton, A.D. In *Drug Discovery Research: New Frontiers in the Post-Genomic Era*, Huang, Z. Ed.; John Wiley & Sons, Inc 2007, pp. 280-298.
4. Chen, L.; Yin, H.; Farooqi, B.; Sebti, S.; Hamilton, A.D. and Chen, J. *Mol Cancer Ther* 2005, **4**(6), 1019-1025.
5. Vassilev, L.T.; Vu, B.T.; Graves, B.; Carvajal, D.; Podlaski, F.; Filipovic, Z.; Kong, N.; Kammlott, U.; Lukacs, C.; Klein, C.; Fotouhi, N.; Liu, E.A. *Science* 2004, **303**, 844-848.
6. Saraogi, I.; Hamilton, A.D. *Biochem.Soc.Trans* 2008, **36**, 1414-1417.
7. Bullock, B.N.; Jochim, A. L. and Arora, P.S. *J. Am. Chem. Soc.* 2011, **133**, 14220-14223.
8. Fry, D.; Huang, K.S.; Lello, P.D.; Mohr, P., Muller, K.; So, S.S.; Harada, T.; Stahl, M.; Vu, B.; Mauser, H. *ChemMedChem Communications* 2013, **8**, 5, 726-732.
9. C.P. Gomes, A.Metz, J.W. Bats, H. Gohlke, M.W. Gobel. *Eur. J. Org. Chem.*, 2012, **77**, 3279-3277
10. Ehlers, I.; Maity, P.; Aubé, J. and König, B. *Eur. J. Org. Chem.* 2011, 2474-2490.
11. Higuieruelo, A.P.; Schreyer, A.; Bickerton, G.R.J.; Pitt, W.R.; Groom, C.R.; Blundell, T.L. *Chem. Biol. Drug Des.* 2009, **74**, 457-460.
12. Deng, X.; Mani, N. S. *J. Org. Chem.* 2008, **73**, 2412-2415.
13. X. Deng, X.; Mani, N.S. *Org. Lett.* 2006, **8**, 16, 3505-3508.
14. Reynes, C.; Host, H.; Camproux, A.-C.; Laconde, G.; Leroux, F.; Mazars A.; Deprez, B.; Fahraeus, R.; Villoutreix, B.O.; Sperandio, O. *PLoS Computational Biology* 2010, **6**, 3, 1-15.
15. Sperandio, O.; Reynes, C.H.; Camproux, A.-C.; Villoutreix, B.O. *Drug Discovery Today* 2010, **15**, 220-229.
16. Neugebauer, A.; Hartmann, R.W.; Klein, C.D. *J. Med. Chem.* 2007, **50**, 4665-4668.

17. Schon, O.; Friedler, A.; Bycroft, M.; Freund, S. M. V.; Fersht, A. R. *J. Mol. Biol.* 2002, **323**, 491-501.
18. Fry, D. C.; Wartchow, C.; Graves, B.; Janson, C.; Lukacs, C.; Kammlott, U.; Belunis, C.; Palme, S.; Klein, C.; Vu, B. *ACS Med. Chem. Lett.* 2013, **4**, 660-665.
19. Molecular Operating Environment (MOE), Chemical Computing Group Inc., 1010 Sherbrooke Street West, Suite 91, Montreal, H3A 2R7, Canada.

Figure 2. Two modes of interaction assumed for compounds of the new scaffold with i, i+4 and i+7 subpockets

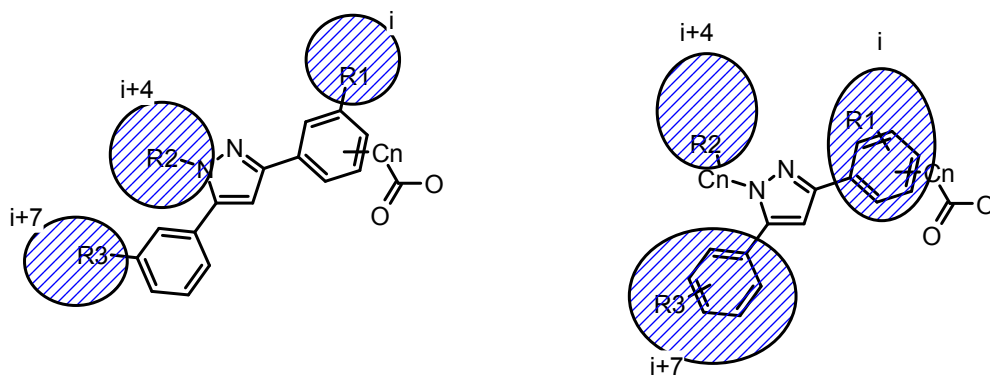
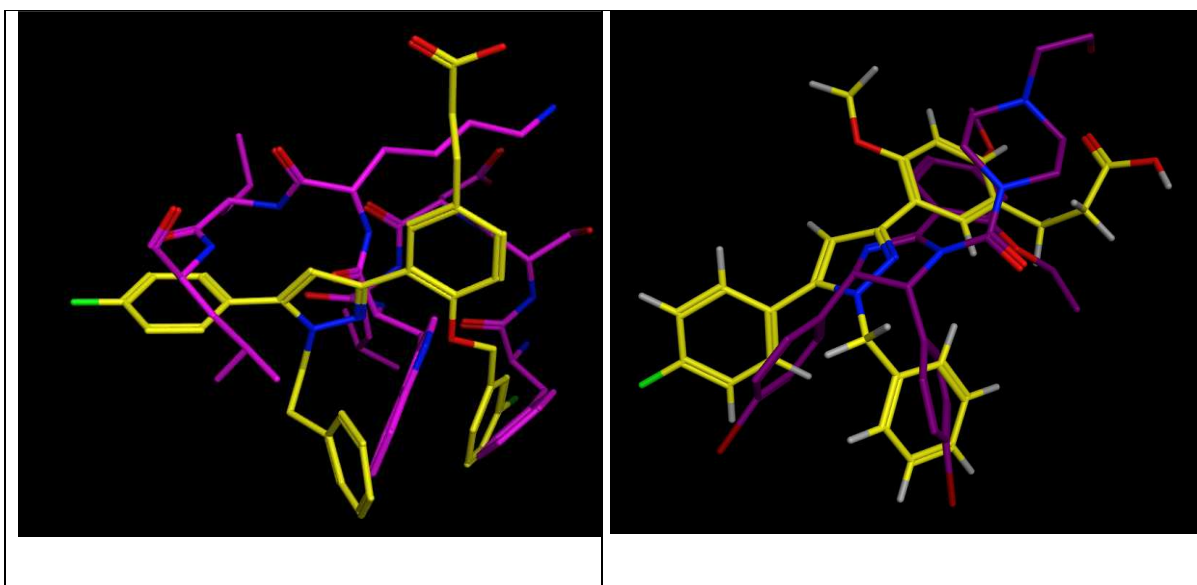


Figure 3. Docking of compounds 8 and 13 into the MDM2 p53 binding site. Left pane: Compound 13 was docked into the p53 binding site of PDB entry 1ycr. Compound 13 (yellow) and transactivation domain of p53 from this entry (purple) are shown. Right pane: Compound 8 was docked into the same complex as in the left pane. MDM2, with 8 docked into it, was then superposed onto the MDM2 complex with nutlin-2 (PDB entry 1rv1). Compound 8 (yellow) and nutlin-2 (purple) are shown.



Scheme 1. Synthetic scheme for the preparation of phenyl-pyrazole-phenyl based compounds.

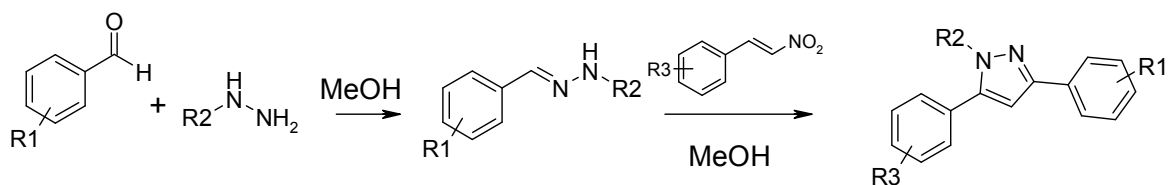
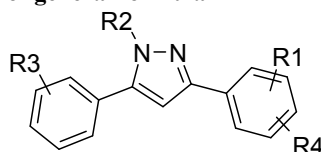


Table 1. Biological data for compounds of general formula



nn	R1	R2	R3	R4	MDM2/p53, IC ₅₀ μM	LE	Solubility, Ug/mL
1	2-OC ₃ H ₇	-C ₂ H ₄ Ph	2-OMe, 3-OMe	5-COOH	6.56	0.20	0.117
2	2-OCH ₂ CH(CH ₃) ₂	-C ₂ H ₄ Ph	2-OMe, 3-OMe	5-COOH	8.22	0.19	0.056
3	2-OEt	-C ₂ H ₄ Ph	2-OEt	5-COOH	10.65	0.21	0.022
4	2-OEt	-C ₂ H ₄ Ph	2-OMe, 3-OMe	5-COOH	13.98	0.20	>0.2
5	2-OC ₄ H ₉	-C ₂ H ₄ Ph	2-OMe, 3-OMe	5-COOH	14.15	0.19	0.066
6	2-OCH ₂ CH(CH ₃) ₂	-C ₂ H ₄ Ph	2-OEt	5-COOH	14.19	0.19	0.015
7	2-OC ₄ H ₉	-C ₂ H ₄ Ph	2-OEt	5-COOH	16.75	0.19	0.032
8	2-OMe	-CH ₂ Ph	4-F	5-C ₂ H ₄ COOH	16.98	0.21	0.066
9	2-OCH ₂ (3-Cl-Ph)	-CH ₂ Ph	2-OMe, 3-OMe	5-C ₂ H ₄ COOH	31.62	0.15	<0.015
10	2-OCH ₂ (3-Cl-Ph)	-C ₂ H ₄ Ph	2-OMe, 3-OMe	5-C ₂ H ₄ COOH	34.02	0.15	<0.015
11	2-OEt	-C ₂ H ₄ Ph	4-F	5-C ₂ H ₄ COOH	35.78	0.18	>0.2
12	2-OMe	-C ₂ H ₄ Ph	4-Cl	5-C ₂ H ₄ COOH	38.87	0.19	0.046
13	2-OCH ₂ (3-Cl-Ph)	-C ₂ H ₄ Ph	4-F	5-C ₂ H ₄ COOH	47.83	0.15	<0.015
14	2-OCH ₂ CH(CH ₃) ₂	-C ₂ H ₄ Ph	2-OEt	5-CH ₂ COOH	48.7	0.16	0.046
15	2-OCH ₂ (3-Cl-Ph)	-CH ₂ Ph	4-F	5-C ₂ H ₄ COOH	51.88	0.16	<0.015
16	2-OC ₄ H ₉	-C ₂ H ₄ Ph	2-OEt	5-CH ₂ COOH	54.06	0.16	0.096
17	2-OCH ₂ (3-Cl-Ph)	-CH ₂ Ph	2-OEt	5-CH ₂ COOH	54.39	0.15	<0.015
18	2-OC ₃ H ₇	-C ₂ H ₄ Ph	2-OMe, 3-OMe	5-CH ₂ COOH	60.6	0.16	0.117
19	2-OCH ₂ CH(CH ₃) ₂	-C ₂ H ₄ Ph	2-OMe, 3-OMe	5-CH ₂ COOH	68.32	0.15	0.056
20	2-OC ₃ H ₇	-CH ₂ Ph	2-OEt	5-COOH	68.75	0.17	0.096
21	2-OC ₃ H ₇	-C ₂ H ₄ Ph	2-OEt	5-CH ₂ COOH	71.98	0.16	0.066
22	2-OC ₃ H ₇	-CH ₂ Ph	2-OMe, 3-OMe	5-COOH	79.27	0.17	>0.2
23	2-OMe	-CH ₂ Ph	4-Cl	5-C ₂ H ₄ COOH	86.63	0.18	0.019
24		-C ₂ H ₄ Ph	2-OEt	4-COOH	91.22	0.18	>0.2
25	2-OEt	-CH ₂ Ph	4-F	5-C ₂ H ₄ COOH	100.8	0.17	<0.015
26	2-OEt	-C ₂ H ₄ Ph	2-OEt	5-CH ₂ COOH	102.4	0.16	>0.2
27	2-OEt	-C ₂ H ₄ Ph	2-OEt	5-C ₂ H ₄ COOH	105.4	0.16	0.102
28	2-OEt	-C ₂ H ₄ Ph	2-OEt	5-COOH	111.1	0.17	0.066
29	2-OC ₄ H ₉	-C ₂ H ₄ Ph	2-OMe, 3-OMe	5-CH ₂ COOH	115.6	0.15	0.117
30	2-OC ₄ H ₉	-CH ₂ Ph	2-OMe, 3-OMe	5-CH ₂ COOH	117.7	0.15	>0.2
31	2-OCH ₂ CH(CH ₃) ₂	-CH ₂ Ph	2-OMe, 3-OMe	5-CH ₂ COOH	120.0	0.15	>0.2
32		-C ₂ H ₄ Ph	4-F	4-COOH	127.9	0.2	0.096
33	2-OCH ₂ (2-Cl-Ph)	-CH ₂ Ph	4-F	5-CH ₂ COOH	129.8	0.14	<0.015
34	2-OMe	-C ₂ H ₄ Ph	2-OMe, 3-OMe	5-COOH	185.6	0.15	>0.2
35	2-OMe	-C ₂ H ₄ Ph	2-OEt	5-COOH	232.5	0.16	>0.2
36	2-OMe	-CH ₂ Ph	2-OEt	5-COOH	238	0.16	0.039
37	2-OCH ₂ (3-Cl-Ph)	-C ₂ H ₄ Ph	2-OEt	5-CH ₂ COOH	248.8	0.12	<0.015
38	2-OMe	-C ₂ H ₄ Ph	2-OEt	5-C ₂ H ₄ COOH	258.4	0.14	>0.2

39	2-OMe	-CH ₂ Ph	2-OEt	5-CH ₂ COOH	287.6	0.15	0.138
40	2-OEt	-CH ₂ Ph	2-OMe, 3-OMe	5-COOH	294.5	0.15	0.138
41	2-OC ₃ H ₇	-CH ₂ Ph	2-OMe, 3-OMe	5-CH ₂ COOH	328.6	0.14	>0.2
42	2-OMe	-C ₂ H ₄ Ph	2-OEt	5-CH ₂ COOH	339.2	0.14	>0.2
43		-CH ₂ Ph	2-OEt	4-COOH	346.4	0.16	0.117
44	2-OEt	-CH ₂ Ph	2-OMe, 3-OMe	5-CH ₂ COOH	348.2	0.14	>0.2
45	2-OEt	-CH ₂ Ph	2-OMe, 3-OMe	5-C ₂ H ₄ COOH	352.7	0.14	>0.2
46	2-OMe	-CH ₂ Ph	2-OEt	5-C ₂ H ₄ COOH	388.1	0.14	>0.2
47	2-OMe	-C ₂ H ₄ Ph	2-OMe, 3-OMe	5-C ₂ H ₄ COOH	436.5	0.13	>0.2
48	2-OMe	-CH ₂ Ph	2-OMe, 3-OMe	5-C ₂ H ₄ COOH	449.2	0.14	0.169
49	2-OMe	-CH ₂ Ph	4-F	5-CH ₂ COOH	594.7	0.15	>0.2
50	2-OMe	-C ₂ H ₄ Ph	2-OMe, 3-OMe	5-CH ₂ COOH	726.8	0.13	>0.2
51	2-OMe	-CH ₂ Ph	2-OMe, 3-OMe	5-CH ₂ COOH	967.3	0.13	>0.2
52	2-OMe	-CH ₂ Ph	2-OMe, 3-OMe	5-COOH	1018.0	0.13	>0.2
Nutlin-3					0.474	0.22	

Abstract

A new class of alpha-helix mimetics, based on the phenyl-pyrazole-phenyl (6-5-6) system, has been designed and synthesized. The ability of the new compounds to inhibit PPIs was confirmed using an MDM2-p53 binding assay. The library, containing completely new compounds, revealed an excellent hit rate of 15%, had satisfactory physico-chemical properties (~38% soluble compounds), and the ligand efficiency of the best compound was 0.21 (0.22 for nutlin-3 in the same assay). Dual mode of action of these inhibitors was suggested based on computer modeling: depending on the nature of their substituents they could act as either an alpha-helix backbone mimetic or an alpha-helix binding epitope mimetic.

Graphical abstract

